Korean J. Chem. Eng., **31**(12), 2251-2260 (2014)
DOI: 10.1007/s11814-014-0185-1

pISSN: 0256-1115
eISSN: 1975-7220

Development of electrolyte SAFT-HR equation of state for single electrolyte solutions

Azam Najafloo*, Farzaneh Feyzi*,†, and Ali Taghi Zoghi**

*Thermodynamics Research Laboratory, School of Chemical Engineering,
Iran University of Science and Technology, Tehran 16846-13114, Iran
**Research Institute of Petroleum Industries, Tehran 14665-1998, Iran

(*Received 14 February 2014 • accepted 1 July 2014*)

Abstract−The explicit version of the mean spherical approximation (MSA) is added to the SAFT-HR equation of state (EoS) to model aqueous alkali halide solutions. The proposed electrolyte equation of state (eEoS) has two parameters per each ion. Two methods are in common use for calculating ion parameters: ion-based and salt-based. In this work, the electrolyte parameters are obtained for 61 single electrolyte solutions using salt-based method. Using this approach, mean ionic activity coefficients of the 61 aqueous electrolyte systems were modeled with overall average absolute relative percent deviation (AAD%) of 3.91. Also, for testing the ability of the model in terms of ionic parameters, six salts (NaCl, NaBr, NaI, KCl, KBr and KI) were studied using ion-based method. The liquid densities, osmotic coefficients and salt mean ionic activity coefficients of 6 aqueous electrolyte solutions were modeled with overall AAD% of 0.68, 2.28 and 0.96, respectively.

Keywords: Electrolyte Solutions, SAFT-HR EoS, Mean Spherical Approximation

INTRODUCTION

Due to the presence of electrolyte-containing solutions in many industrial processes, detailed examination of the behavior of such systems, under different conditions of pressure and temperature, is under investigation by many researchers. In many chemical processes, such as acid gas elimination by aqueous solutions of alkanolamines, extractive distillation, enhanced oil recovery, desalination, hydrometallurgy and production of fertilizers, a detailed understanding of the phase equilibria of systems containing electrolytes is needed and, hence, accurate models to describe their thermodynamic properties are required. The existing models could be classified into two categories: activity coefficient models and equations of state (EoS) [1]. All these models commonly combine the Debye-Huckel (DH) or the mean spherical approximation (MSA) models to account for electrostatic interactions combined with an activity coefficient or EoS model that represents the short-range interactions [2]. MSA has two forms: the primitive (PM) [3] and the nonprimitive (NPM) [4]. In the PM model, the solvent is not defined by a molecularly realistic representation, and it is assumed to be a continuous medium through its dielectric constant. If the ions have equal diameters, the approximation is referred to as the restricted primitive model (RPM). In the NPM model, the solvent has a molecularly more realistic definition. Fig. 1 shows the MSA ideas for RPM, PM, and NPM models [5].

The advantages of activity coefficient models are their relative simplicity and their high precision for various electrolyte solutions. However, the inability to calculate the density of the solution and being pressure-independent [6] are their weaknesses. Some of the well-known models in this category are NRTL [7], Pitzer [8], and NRTL-NRF [9]. Since electrolyte EoS models (eEoS) do not have these weaknesses they are usually preferred for phase equilibrium calculations. Numerous eEoSs are proposed in the literature for electrolyte solutions. Planche and Renon [10] developed an eEoS containing a hard sphere, an attractive and an implicit MSA contribution [3,4]. Myers et al. [11] developed an eEoS which uses a volume translated Peng-Robinson EoS combined with explicit MSA and the Born term. Clarke and Bishnoi [12] used modified Peng-Robinson EoS coupled with simplified MSA and a specific term to account for solvation effects. Haghtalab and Mazloumi [6] used electrolyte cubic square-well EoS [13] coupled with explicit version of MSA to predict the mean ionic activity coefficient of strong aqueous electrolyte solutions. In recent years statistical associating fluid theory (SAFT) [14] family of EoS is very popular. To extend the SAFT EoS to electrolyte solutions, usually the MSA model is employed to consider the electrostatic interactions [5]. Galindo et al. [15] and Villegas et al. [16] used the RPM model to account for long-range columbic ion-ion interactions and SAFT-VR EoS for long-range water-water and ion-water attractive interactions. Tan et al. [17] used SAFT1 EoS [18] coupled with RPM to calculate the mean ionic

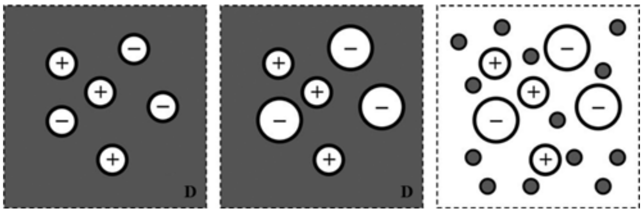

Fig. 1. Mean spherical approximation of aqueous electrolytes: restricted primitive model (left), primitive model (middle) and nonprimitive model (right), where D is the solvent dielectric constant and the small shady circles are solvent molecules [5].

---

† To whom correspondence should be addressed.
E-mail: feyzi@iust.ac.ir

activity coefficient, density, osmotic coefficient, and vapor pressure of some aqueous alkali halide solutions. Ji et al. [19] extended the SAFT1-RPM model [17] for representing multiple-salt solutions in water. Tan et al. [20] and Ji et al. [21] applied SAFT2 EoS [20] to multivalent ions by relaxing the range of the square-well width parameter. Liu et al. [22] coupled the NPM term with SAFT-0 EoS [23], in which a low-density expansion term of NPM is used to account for solvent-solvent and ion-solvent associations. Behzadi et al. [24] applied the PM model to Yukawa SAFT-VR EoS to model seven hydrogen-bonding solvents and 23 electrolyte solutions. Zhao et al. [25] proposed an NPM term to be coupled with SAFT-VR+D EoS [26] to account for ion-dipole, dipole-dipole and ion-ion interactions. Held et al. [27] used the ePC-SAFT EoS proposed by Cameretti et al. [28] to describe thermodynamic properties of several aqueous electrolyte solutions. Herzog et al. [29] used an NPM term coupled with PC-SAFT EoS to model completely dissociating aqueous alkali halide systems. Shahriari et al. [30] used the MSA model coupled PC-SAFT EoS for thermodynamic modeling of aqueous ionic liquid solutions.

In this work, to consider the electrostatic interactions between charged particles, the explicit simple version of MSA model [6] is coupled with SAFT-HR EoS [31,32] proposed by Huang and Radosz. Only two parameters are used to characterize each charged particle. The first one is the temperature-independent segment volume (v^{00}), and the second one is the temperature-independent dispersion energy of interaction between segments (u^0/k_B). The parameters can be obtained using two approaches, ion-based or salt-based. Both of these methods are used in this work for parameter estimation. The new set of parameters is able to reasonably describe the mean ionic activity coefficient of about 61 electrolyte systems.

THEORY

SAFT is an approach to describe associating fluids with Wertheim's theory [33-35]. In contrast to a chemical theory, which assumes hypothetical chemical reactions in the fluid, SAFT and other methods based on statistical mechanics, relate molecular association to intermolecular interactions and are thus considered as a physical approach. The advantage of such physical theories is that they can be tested against molecular simulation results. We have applied SAFT-HR [31,32] to account for short-range forces and the explicit simple version of MSA for long-range interactions between ions in electrolyte solutions. We have called the model as eSAFT-HR EoS.

1. SAFT-HR Equation of State

The SAFT-HR EoS [31,32] is used to describe the non-electrostatic interactions between non-charged and charged molecules in electrolyte solutions, which in terms of the residual Helmholtz energy is presented as follows:

$$\frac{A^{res}}{N_A k_B T}=\frac{A^{hs}}{N_A k_B T}+\frac{A^{disp}}{N_A k_B T}+\frac{A^{chain}}{N_A k_B T}+\frac{A^{assoc}}{N_A k_B T} \qquad (1)$$

A, N_A, and T are the Helmholtz energy, Avogadro's number, Boltzmann's constant and temperature, respectively. Superscripts res, hs, disp, chain and assoc denote residual, hard-sphere, dispersion, chain and association contributions, respectively. Details of the non-electrostatic terms are given in the original work of Huang and Radosz [31,32]. This EoS, in terms of Helmholtz energy, is introduced in Appendix A.

2. The eSAFT EoS

The electrostatic contribution due to the interactions between ions (A^{elec}) is considered using a explicit simple version of MSA model [36], given by Eqs. (2) to (5), which is added to the right hand side of Eq. (1).

$$\frac{A^{elec}}{N_A k_B T}=-\frac{2\Gamma^3}{3\pi\rho}\left(1+\frac{3}{2}\sigma\Gamma\right) \qquad (2)$$

$$\Gamma=\frac{1}{2\sigma}\left[\sqrt{1+2\sigma\kappa}-1\right] \qquad (3)$$

$$\kappa^2=\frac{e^2N_A^2}{D\varepsilon_0 RTv}\sum_{ions} x_i Z_i^2 \qquad (4)$$

$$\sigma=\frac{\sum_{ions} x_i\sigma_i}{\sum_{ions} x_i} \qquad (5)$$

where Γ, ρ, κ, x_i, Z_i, σ_i, ε_0, R and v are the MSA screening parameter, molar density, the Debye screening length, mole fraction of component i, charge number of ionic species i, diameter of ionic species i, vacuum permittivity, gas constant and molar volume, respectively. D is the dielectric constant of the solution and is assumed to be equal to the dielectric constant of water which is calculated from the following expression [37]:

$$D=-19.291+\frac{29815}{T}-0.019678\times T \\ +1.3189\times10^{-4}\times T^2-3.1144\times10^{-7}\times T^3 \qquad (6)$$

A combination of Eqs. (1) and (2) constructs the eSAFT EoS in terms of the Helmholtz energy. Compressibility factor and chemical potential are obtained from the following thermodynamic relations:

$$Z=1+\rho\left(\frac{\partial(A^{res}/Nk_BT)}{\partial\rho}\right)_{T,n} \qquad (7)$$

$$\frac{\mu_i^{res}}{Nk_BT}=\left(\frac{\partial(nA^{res}/Nk_BT)}{\partial n_i}\right)_{T,V,n_{j\neq i}} \qquad (8)$$

Using Eqs. (7) and (8), the compressibility factor and the chemical potential due to electrostatic interactions are obtained as follows:

$$Z^{elec}=\frac{2\Gamma^3}{3\pi\rho}\left(1+\frac{3}{2}\Gamma\sigma\right)-\frac{\kappa^2}{4\pi\rho}\times\frac{\Gamma}{1+\Gamma\sigma} \qquad (9)$$

$$\frac{\mu_i^{elec}}{RT}=\frac{e^2N_AZ_i^2}{4\pi D\varepsilon_0 RT}\times\frac{\Gamma}{1+\Gamma\sigma} \qquad (10)$$

In the above equations e is the unit of elementary charge. The fugacity coefficient of component i in a mixture is obtained from:

$$\ln\varphi_i=\mu_i^{res}-\ln Z \qquad (11)$$

The ion and solvent activity coefficients are calculated from:

$$\gamma_{ion}^{*}=\frac{\varphi_i(T,P,x)}{\varphi_i(T,P,x_{ion}\rightarrow 0)} \qquad (12)$$

$$\gamma_s=\frac{\varphi_s(T,P,x)}{\varphi_s(T,P,x_s\rightarrow 1)} \qquad (13)$$

Subscript s refers to solvent. Then, the mole fraction based mean ionic activity coefficient can be obtained as:

$$\gamma_\pm^x = (\gamma_+^{\nu_+}\gamma_-^{\nu_-})^{1/(\nu_+ + \nu_-)} \tag{14}$$

where $\gamma_\pm^x$ is the mean ionic activity coefficient on mole fraction basis, ν_+ and ν_- are cation and anion stoichiometric coefficients, respectively. The osmotic coefficient ($\Phi^{(m)}$) can be calculated from:

$$\Phi^{(m)} = -1000\frac{\ln(x_s\gamma_s)}{(\nu_+ + \nu_-)M_s m_e} \tag{15}$$

where M_s is the molar mass of the solvent and m_e is the molality of electrolyte.

RESULTS AND DISCUSSION

1. Pure Water

Since water is the main constituent of electrolyte solutions, any thermodynamic model for these solutions must be able to predict the properties of pure water, especially the liquid density due to its direct effect on ion parameters.

Following Huang and Radosz [31,32] we have considered water to have three association sites. Consequently, five parameters are needed to describe the properties of water: the chain length number (m), temperature-independent segment volume (ν^{00}), temperature-independent dispersion energy of interaction between segments (u^0/k_B), the volume of association ($\kappa^{A_iB_j}$) and the energy of association ($\varepsilon^{A_iB_j}$). Huang and Radosz [31] fitted these parameters for water in the temperature range of 283-613 K. The same parameters, that are presented in Table 1, are used in this work.

Table 1. SAFT-HR parameters for pure water in the temperature range of 283-613 K [30]

Parameters				
m	$u^0/k_B/K$	ν^{00}/mL·mol^{-1}	$\varepsilon^{A_iB_j}/k_B/K$	$\kappa^{A_iB_j}$
0.01593	1809	10.0	528.17	1.179

2. Ion Parameters

Two methods are commonly used for calculating ion parameters in modeling electrolyte solutions: ion-based and salt-based [38]. In the ion-based method, the ion parameters are transferable among the same ions in different salts, while in the salt-based method salt parameters are unique to specific salts. In this work, to estimate the ion parameters using the salt-based method, the mean ionic activity coefficient data of 61 electrolyte solutions are correlated using eSAFT-HR EoS at 25 °C and 1 bar. The model has two adjustable parameters for each ion (ν^{00} and u^0/k) which are obtained using the following objective function:

$$OF = \sum_i \frac{\left|\gamma_\pm^{m,exp} - \gamma_\pm^{m,cal}\right|}{\gamma_\pm^{m,exp}} \tag{16}$$

where

$$\gamma_\pm^{m,exp} = \frac{\gamma_\pm^x}{1 + 0.001(\nu_+ + \nu_-)m_e M_s} \tag{17}$$

$\gamma_\pm^{m,exp}$, $\gamma_\pm^{m,cal}$ are, respectively, the experimental and calculated mean ionic activity coefficients based on molality scale and $\gamma_\pm^x$ is calculated from Eq. (14). The optimal values of ν^{00} and u^0/k_B for each

Table 2. The optimized parameters of the eSAFT-HR EoS using salt-based method and comparison of the results with other eSAFT EoS models

Salt	m_{max}[a]/ mol·kg^{-1}	ν_{cation}^{00}/ ml·mol^{-1}	ν_{anion}^{00}/ ml·mol^{-1}	$(u^0/k_B)_{cation}$/ K	$(u^0/k_B)_{anion}$/ K	AAD[b] %			
						This work	Liu et al. [38]	Herzog et al. [28]	Held et al. [26]
HCl	6	99.018	1.078	554.031	2354.306	2.58	3.07		9.8
HBr	3	81.800	3.657	627.817	1046.279	0.91	2.86		9.28
HI	3	29.603	63.771	776.682	608.326	0.93	3.03	5.32	2.56
HNO_3	3	35.133	42.880	648.597	564.729	0.46	2.18		6.87
$HClO_4$	6	22.505	112.177	620.178	526.765	4.35	0.63		9.02
LiCl	6	55.559	1.969	1008.175	258.118	3.19	3.07	8.43	9.79
LiBr	6	59.181	1.758	1041.370	173.780	4.88	1.67	4.41	3.52
LiI	6	36.175	29.472	1093.056	626.063	1.39	0.50	3.47	4.49
$LiNO_3$	3	51.453	1.879	1155.949	296.885	1.41	2.45		14.25
$LiClO_4$	4	9.324	61.561	703.611	788.575	1.44			
NaF	1	10.205	43.116	625.930	2017.553	0.07	3.65	5.51	2.38
NaCl	6	35.496	9.626	733.241	813.743	1.38	2.71	5.00	3.43
NaBr	4	20.274	28.714	726.079	699.965	0.60	2.02	2.36	1.75
NaI	3.5	18.537	32.115	655.628	1078.375	0.67	2.05	4.98	1.37
$NaNO_3$	6	31.730	39.087	531.091	541.510	0.33	1.73		1.99
$NaClO_4$	6	10.620	32.844	1096.464	960.204	1.12	0.82		14.14
$NaClO_3$	3.5	29.901	39.337	570.839	534.822	0.45	1.54		2.14
KF	4	37.286	6.857	769.454	666.606	0.52	3.37		3.26
KCl	5	24.888	15.395	655.209	560.228	0.52	2.10	3.35	2.38
KBr	5.5	17.774	25.367	593.330	621.213	0.53	2.21	3.78	1.78

Table 2. Continued

Salt	$m_{max}{}^{a}$/ mol·kg^{-1}	v^{00}_{cation} / ml·mol^{-1}	v^{00}_{anion} / ml·mol^{-1}	$(u^0/k_B)_{cation}$/ K	$(u^0/k_B)_{anion}$/ K	AAD^b %			
						This work	Liu et al. [38]	Herzog et al. [28]	Held et al. [26]
KI	4.5	19.306	34.535	733.579	552.908	0.53	1.66	2.85	1.44
KNO_3	3.5	8.461	38.995	1070.281	489.531	0.32	0.87		2.28
$KClO_3$	0.7	14.432	36.780	517.939	507.996	0.51	1.69		0.96
RbF	0.2	11.233	40.080	757.842	772.605	0.04	4.34	3.00	6.7
RbCl	5	9.792	23.738	847.966	742.502	0.27	1.31	4.87	1.35
RbBr	5	15.158	18.150	977.839	787.070	0.23	1.46	4.20	1.89
RbI	5	10.303	21.958	918.667	694.621	0.26	1.88	9.17	3.3
$RbNO_3$	4.5	10.791	1.307	602.811	1040.550	0.40	1.82		2.92
CsF	0.2	7.951	82.940	465.372	2890.742	0.13	3.50	3.11	6.39
CsCl	6	31.091	0.656	929.528	109.054	0.38	1.17	7.94	1.91
CsBr	5	2.741	31.103	222.950	968.618	0.29	1.26	7.39	2.56
CsI	3	4.106	23.606	654.113	826.272	0.12	0.31	6.81	4.66
$CsNO_3$	1.4	12.088	70.675	541.179	623.145	0.13	1.51		3.68
$CaCl_2$	3	81.627	20.734	629.9855	988.850	13.15			26.11
$CaBr_2$	4	50.627	47.518	635.6928	812.364	6.63			18.31
CaI_2	2	25.394	56.548	739.5189	1046.411	1.91			10.15
$BaCl_2$	1.8	52.233	58.584	513.4519	657.789	8.98			5.68
$BaBr_2$	2	51.192	44.834	1024.781	457.384	7.41			6.47
BaI_2	2	22.474	56.328	953.1443	1478.862	7.23			9.46
K_2CrO_4	1	65.921	25.649	486.3744	1141.642	6.00			
Na_2SO_4	4	30.848	62.554	535.3663	504.340	5.95			32.63
Na_2CrO_4	4	57.658	18.394	550.4072	589.937	8.71			
$MgCl_2$	5	95.265	27.752	558.1807	889.834	8.23			11.08
$MgBr_2$	5	72.706	41.467	773.0217	654.512	7.93			13.43
MgI_2	5	50.242	51.786	769.7411	861.667	8.64			47.18
$SrCl_2$	4	54.870	43.669	463.7234	1107.888	6.04			11.05
$SrBr_2$	2	62.199	43.495	476.7357	1019.464	6.21			11.91
SrI_2	2	67.388	48.961	483.5388	978.462	6.83			11.26
$CuBr_2$	0.2	66.037	47.486	767.775	1005.604	5.58			18.38
$CuCl_2$	6	28.787	46.834	435.345	1137.492	10.18			19.52
$Cu(NO_3)_2$	3	25.363	42.363	593.322	1632.623	8.72			32.96
$Cu(ClO_4)_2$	0.2	50.215	61.144	832.148	1106.710	5.80			25.66
$FeCl_2$	1	49.305	64.802	533.920	710.927	6.88			7.13
$NiCl_2$	1	46.183	70.938	533.642	700.509	6.79			
$Ni(NO3)_2$	0.2	33.280	101.211	545.175	696.951	4.77			
$NiBr_2$	0.2	53.480	98.804	544.493	713.044	4.96			
$Ni(CLO_4)_2$	0.2	60.840	135.585	585.953	621.667	5.45			
$CoCl_2$	4	47.834	63.033	534.841	701.709	6.78			12.10
$CoBr_2$	5	53.505	54.151	782.410	684.073	10.20			8.55
CoI_2	4	43.927	67.409	625.527	801.146	10.90			10.62
$Co(NO_3)_2$	5	52.193	58.464	547.541	688.584	8.80			15.92

$^a m_{max}$ is the maximum molality of the salt in electrolyte solution

$$^b\mathrm{AAD\%} = \frac{1}{n}\sum_i \frac{\gamma_{\pm}^{m,exp} - \gamma_{\pm}^{m,cal}}{\gamma_{\pm}^{m,exp}} \times 100$$

ion of a salt are listed in Table 2. Moreover, Table 2 gives the comparison of the results of this work with that of Liu et al. [39] who used the NPM MSA model coupled with SAFT EoS [14] for calculating mean ionic activity coefficients of 46 single 1 : 1 electrolytes. In their work they considered cation and anion diameters as adjustable parameters for each electrolyte. Based on the overall AAD% observed in Table 2, the results of eSAFT-HR EoS show better agreement with experimental data than the results of Liu et al. [39], in which the maximum electrolyte concentration is 3.0 mol/kg for each aqueous electrolyte solution. In this work, in most cases, the maximum electrolyte concentrations are higher than 3 mol/kg. It can be seen that for 84.85% of the electrolytes considered, eSAFT-HR EoS presents more accurate results in comparison to the results reported by Liu et al. [39]. As mentioned in the introduction section, Herzog et al. [29] used a semirestricted NPM model in combination with the PC-SAFT EoS for aqueous electrolyte solutions. They used ePC-SAFT EoS for correlation of the mean ionic activity coefficients of 19 binary aqueous electrolyte solutions at 25 °C. Held et al. [27] used the ePC-SAFT EoS proposed by Cameretti et al. [28] to describe the mean ionic activity coefficients of 115 aqueous electrolyte solutions. The results of this work are also compared with the results of Herzog et al. [29] and Held et al. [27] in Table 2. As can be seen, the AAD% of our model for 74.42% of the electrolytes considered is less than the AAD% of Held et al. [27]. Also, for 94.74% of electrolytes the new eEoS is more accurate than the results of Herzog et al. [29].

As may be concluded from the above comparisons, the explicit simple version of MSA model, used in this work, has produced more accurate results in comparison with the NPM MSA model used by Liu et al. [39] and Herzog et al. [29]. In the PM MSA model, only the electrostatic interactions between ions are considered and the ion-solvent and solvent-solvent interactions are accounted for via the solvent dielectric constant (D) in the electrostatic term. In the NPM MSA model, the solvent molecules are treated as interacting particles. Lu et al. [40] used the modified PM MSA model to correlate the mean ionic activity coefficients of 85 single-electrolyte solutions. They showed that the modified PM MSA model gives smaller deviations in comparison to the NPM MSA. The NPM MSA model is not suc- cessful for asymmetric electrolytes [41]. Li [42], by comparing the PM MSA and the NPM MSA models, concluded that the PM MSA is more accurate and simpler for practical use. Maybe the values of the radial distribution function for cation-cation with large size difference become negative, which is an unphysical feature of the NPM MSA approach [43]. Also, Lee [43] showed that the short-range electrostatic term of the NPM MSA always has a negative contribution, while the corresponding part of Pitzer's formulation is positive. The success of Pitzer's correlation strongly suggests the desirability of a positive electrostatic contribution. Moreover, replacing RPM by PM does not improve the EoS performance [5].

It is observed in Table 2 that the eSAFT-HR EoS has performed well in modeling the mean ionic activity coefficient for the majority of the electrolyte solutions. For better presentation of the results, the calculated mean ionic activity coefficients of a few electrolyte solutions are depicted in Figs. 2-4, which show that the results of the new EoS are in good agreement with the experimental data. Fig. 2 shows the calculated mean ionic activity coefficients of HCL, HBr and HI electrolyte solutions at 25 °C. The results for HCl show that

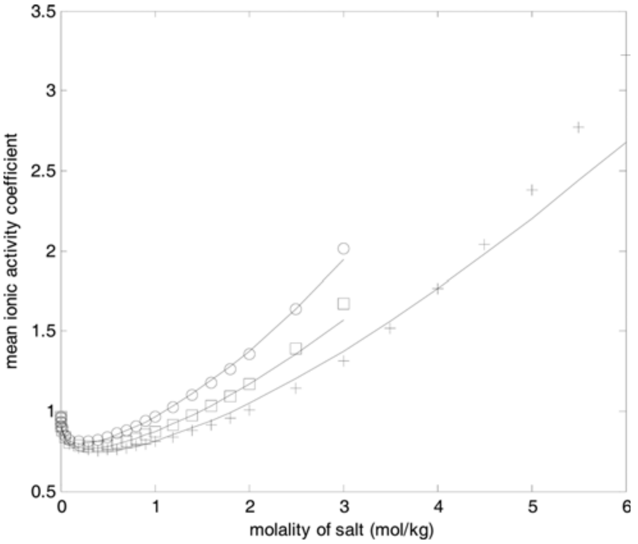

Fig. 2. The mean ionic activity coefficients of aqueous solutions of halogen halides at 298.15 K, the data: [39]. HCl: +, HBr: □, HI: ○, eSAFT-HR EoS: line.

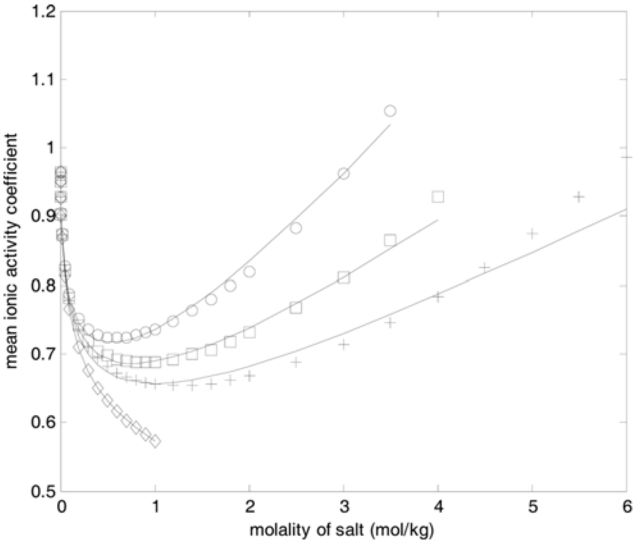

Fig. 3. The mean ionic activity coefficients of aqueous solutions of four sodium salts at 298.15 K, the data: [39]. NaF: ◇, NaCl: +, NaBr: □, NaI: ○, eSAFT-HR EoS: line.

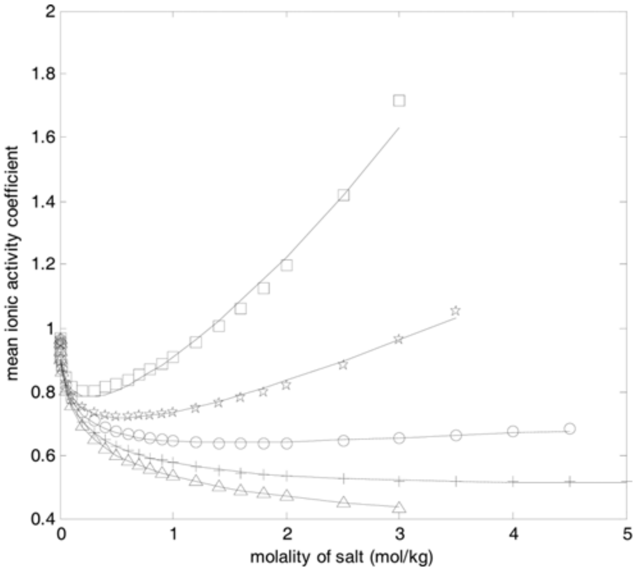

Fig. 4. The mean ionic activity coefficients of aqueous solutions of five iodide salts at 298.15 K, the data: [39]. LiI: □, NaI: ☆, KI: ○, RbI: +, CsI: △, eSAFT-HR EoS: line.

at concentrations less than 4 mol/kg the estimated values of the mean ionic activity coefficients are obtained with high accuracy. However, at concentrations above 4 mol/kg the estimated values of the mean ionic activity coefficient are lower than the experimental values. The reason is that the non-idealities of electrolyte solutions increase with increasing electrolyte concentration. As can also be seen in Fig. 2, mean ionic activity coefficient values first decrease and then, after reaching a minimum, increase with increasing the salt concentration. This phenomenon is an evidence of extensive hydration [44]. In the case of HBr and HI at concentrations up to 2.5 mol/kg the values of the mean ionic activity coefficient are obtained with excellent accuracy. In Fig. 3, the hydration of F^-, Cl^-, Br^- and I^- is compared. The following sequence is observed: $\gamma^m_{\pm,NaI}>\gamma^m_{\pm,NaBr}>\gamma^m_{\pm,NaCl}>\gamma^m_{\pm,NaF}$, which shows the salt with the smallest anion has the minimum mean ionic activity coefficient, and as the size of the anion increases the mean ionic activity coefficient increases. A probable description for this reverse behavior is the so-called localized hydrolysis [45]. A strong proton acceptor anion (like F^-) will "dock" at the hydration shell to form an acid with the respective proton. As a result, the water molecule is split up to form the acid of the anion and the hydroxide of the cation:

$$\text{Cation}^+\ldots\text{OH}^- - \text{H}^+ + \text{F}^- \rightarrow \text{Cation}^+\ldots\text{OH}^- + \text{H}^+\ldots\text{F}^-$$

As a result, the efficient number of the ions in the solution is decreased. Decreasing the number of ions leads to decreasing the mean ionic activity coefficient values. Another interesting effect can be observed for the alkali metal iodides shown in Fig. 4, which also shows the hydration of ions. As can be seen in this figure the following result is achieved:

$$\gamma^m_{\pm,LiI}>\gamma^m_{\pm,NaI}>\gamma^m_{\pm,KI}>\gamma^m_{\pm,RbI}>\gamma^m_{\pm,CsI}$$

Indeed, the smallest alkali cation has the highest surface charge density and is highly hydrated. Strong hydration results in high mean ionic activity coefficient values. The calculation results with eSAFT-HR EoS for the mean ionic activity coefficient series in Fig. 4 follow the similar trend as the experimental data with very good accuracy.

For testing the potential of the model in terms of the ionic parameters, six salts (NaCl, NaBr, NaI, KCl, KBr and KI) have been studied using ion-based method. In this method the ion parameters are adjusted by simultaneous regression of experimental data on liquid solution densities and mean ionic activity coefficients. The following objective function is used for adjusting ion-specific parameters:

$$\mathrm{OF}=\sum_{i=1}^{N_s}\sum_{j=1}^{N_p}\left[\left(\frac{\gamma^{m,exp}_{\pm,j}-\gamma^{m,cal}_{\pm,j}}{\gamma^{m,exp}_{\pm,j}}\right)^2+\left(\frac{\rho^{exp}_j-\rho^{cal}_j}{\rho^{exp}_j}\right)^2\right]_i \tag{18}$$

N_s and N_p are the number of the electrolyte solutions and the number of data points for each solution, respectively. Experimental data on electrolyte solutions' density have been used from Novotny and Sohnel [46], and the mean ionic activity coefficient data are taken from Robinson and Stokes [44]. To minimize the mentioned objective function, ten parameters have been adjusted simultaneously. The Nelder-Mead simplex method is used for the optimization algorithm [47]. The results are presented in Table 3. It is observed that the proposed model is able to correlate the mean ionic activity coefficients and liquid densities of alkali halide electrolyte solutions with suitable accuracy. According to the results the minimum and maximum AAD% for liquid density are 0.11 and 1.31, and for mean ionic activity coefficient are 0.54 and 1.59, respectively. It is also observed that the dispersion energy parameter of anions and cations decrease with increasing their diameter. The reason is that with increasing the size of the ions, their charge density decreases and thus their interaction with each other and with the solvent molecule is weakened. Using the parameters summarized in Table 3, liquid densities are calculated. As a typical example, Fig. 5 shows the calculated liquid densities of KCl, KBr and KI electrolyte solutions compared to experimental data. Good agreement between the calculated and experimental data is evident.

Table 3. Ion parameters obtained for eSAFT-HR EoS using ion-based method and the AAD% of the mean ionic activity coefficient ($\gamma^m_\pm$), osmotic coefficient ($\Phi^{(m)}$) and solution density (ρ) at 298.15 K and 1 bar

Ion	Parameters		Salt	m_{max}/ $\mathrm{mol\cdot kg^{-1}}$	AAD%[a]		
	ν^{00} / $\mathrm{ml\cdot mol^{-1}}$	u^0/k_B/K			ρ	$\gamma_\pm^m$	$\Phi^{(m)}$
			NaCl	6	1.31	1.51	2.59
Na^+	32.593	1498.122	NaBr	4	0.85	1.59	2.27
K^+	26.971	1251.944	NaI	3.5	0.67	0.93	2.39
Cl^-	13.937	416.537	KCl	5	0.55	0.61	2.23
Br^-	15.031	415.851	KBr	5.5	0.59	0.59	2.21
I^-	17.534	353.855	KI	4.5	0.11	0.54	1.97
				Average	0.68	0.96	2.28

[a] Average absolute relative percent deviation (AAD%) $=\frac{1}{n}\sum_{i=1}^{n}\left|\frac{\mathrm{calc}-\mathrm{exp}}{\mathrm{exp}}\right|\times 100$

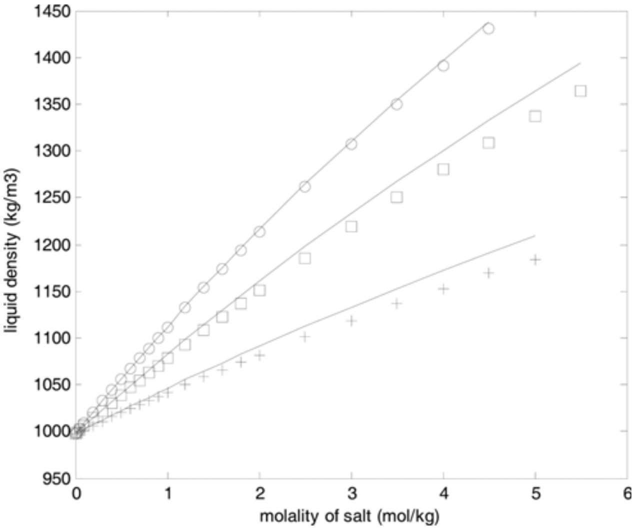

Fig. 5. Comparison between the correlated and experimental liquid density for aqueous solutions of three potassium salts at 298.15 K. Experimental data [41]: KCl: +, KBr: □, KI: ○; eSAFT-HR EoS: line.

To further check the accuracy of the model, osmotic coefficients of NaCl, NaBr, NaI, KCl, KBr and KI electrolyte solutions are calculated and given in Table 3. As a typical example, Fig. 6 shows the calculated osmotic coefficients of NaCl, NaBr and NaI electrolyte solutions compared to experimental data. As can be seen, the

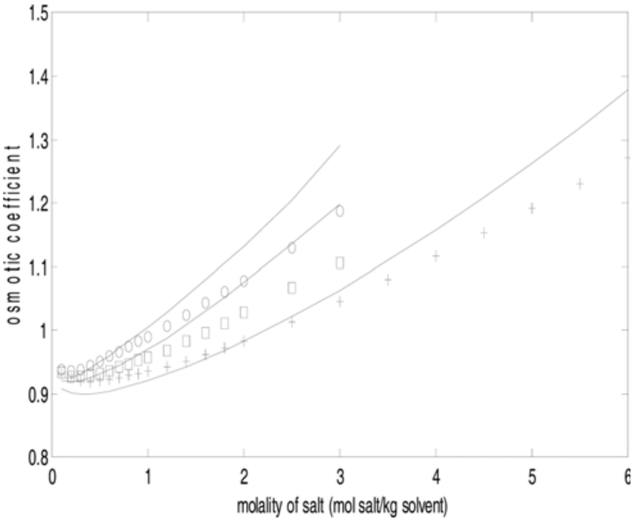

Fig. 6. Comparison between the correlated and experimental osmotic coefficient for three sodium salts at 298.15 K. Experimental data [39]: NaCl: +, NaBr: □, NaI: ○; eSAFT-HR EoS: line.

Table 4. Comparison between calculated ion diameters using eSAFT-HR EoS and Crystal diameters

Ion	σ/Å	Crystal diameters [37]
Na^+	4.25	1.98
K^+	3.99	2.66
Cl^-	3.20	3.60
Br^-	3.28	3.89
I^-	3.45	4.12

experimental data are modeled with high accuracy even at high salt concentrations of up to 6 mol/kg. The results of Table 3 show that for NaCl, NaBr, NaI, KCl, KBr and KI electrolyte solutions the AAD% for the osmotic coefficient is 2.28.

The ionic diameter is also calculated by the following equation using the parameters of eSAFT-HR EoS and the results are compared with the crystal diameter:

$$\sigma=\left(\frac{6\tau}{\pi N_A}v^{00}\right)^{1/3} \tag{19}$$

where τ=0.74048. The results are given in Table 4: the adjusted diameters of the cations are larger than the corresponding crystal diameters, while for anions no significant difference is observed. This result is an indication of the strong hydration capacity due to high charge density of cations.

Tan et al. [17] have developed an e-SAFT EoS extension of their SAFT variant, called SAFT1. They used the RPM version of MSA. The parameter estimation was the novelty of their approach. They have developed a hybrid approach using ion-specific parameters with three adjustable parameters: ion segment dispersion energy, ion segment volume and the range of the square-well potential. In Table 5 the AAD% for liquid density and mean ionic activity coefficient of SAFT1 EoS are 0.39 and 0.31, respectively.

Ji et al. [48] developed SAFT2 EoS, which is based on a hybrid approach for the parameter calculation of ions. In SAFT2 EoS, a new dispersion term is developed because the range of the square-well width parameter is relaxed. Each ion has four parameters: ion segment dispersion energy, ion segment volume, reduced well range for square-well potential and effective diameter. Results of this model are also presented in Table 5.

In addition to the works of Tan et al. [17] and Ji et al. [48], the present ion based model is compared with the works of Herzog et al. [29] and Held et al. [27] in Table 5. As can be seen from this table, the AAD% for liquid density and mean ionic activity coefficient of this work are 0.68 and 0.96, respectively. The error values calculated by the present model are comparable with other models and in some cases, the error is even less. For example, for all the six salts the AAD% of mean ionic activity coefficient of this work is less than the work of Herzog et al. [29]. The AAD% of mean ionic activity coefficient of our model for 66.67% of electrolytes is less than that of the work of Held et al. [27]. However, for prediction of density the new eEoS is less accurate than the results of Held et al. [27]. The result of Tan et al. [17] is better than the results of this work with more adjustable ionic parameters. Compared with the work of Ji et al. [48], for prediction of density, the new eEoS is

Table 5. AAD% of the calculated density (ρ) and the mean ionic activity coefficient ($\gamma_\pm^m$) of the eSAFT-HR EoS using ion-based method and four different models based on the SAFT equation of state

	This work (SAFT-HR)		Herzog et al. (PC-SAFT) [28]		Held et al. (PC-SAFT) [26]		Tan et al. (SAFT 1) [17]		Ji et al. (SAFT 2) [42]	
Number of adjustable ionic parameters	2		2		2		3		4	
Salt	ρ	$\gamma_\pm^m$	ρ	$\gamma_\pm^m$	ρ	$\gamma_\pm^m$	ρ	$\gamma_\pm^m$	ρ	$\gamma_\pm^m$
NaCl	1.31	1.51	-	5	0.74	3.43	0.38	0.55	0.47	0.41
NaBr	0.85	1.59	-	2.36	0.46	0.25	0.35	0.52	1.75	1.03
NaI	0.67	0.93	-	4.98	0.45	1.14	0.29	0.34	1.37	0.52
KCl	0.55	0.61	-	3.35	0.38	0.63	0.48	0.18	2.38	0.49
KBr	0.59	0.59	-	3.78	0.32	0.31	0.45	0.08	1.78	0.56
KI	0.11	0.54	-	2.85	0.57	0.74	0.37	0.17	1.44	0.16
Average deviation	0.68	0.96	-	3.72	0.49	1.08	0.39	0.31	1.53	0.53

more accurate with fewer adjustable ionic parameters.

CONCLUSION

SAFT-HR EoS has been coupled by explicit simple version of MSA model to account for the electrostatic interactions between charged ions for 61 single electrolyte solutions. For this purpose two adjustable parameters have been employed for each ion. The model parameters were obtained using two methods, ion-based and salt-based. In the ion based approach, the obtained parameters are universal and can be used for different salts containing the same ions. In this work, the ion-based approach has been utilized for six salts: NaCl, NaBr, NaI, KCl, KBr and KI. With this approach, liquid densities, osmotic coefficients and salt mean ionic activity coefficients of six aqueous electrolyte solutions were modeled reasonably with overall AAD% of 0.68, 2.28 and 0.96, respectively. Also the salt-based approach was used to obtain 61 salts ionic parameters. By this approach, salt mean activity coefficients of 61 aqueous electrolyte systems were modeled with overall AAD% of 3.91.

LIST OF SYMBOLS

A : Helmholtz energy
D : dielectric constant of solution
e : electronic charge ($1.60219\times10-19$ C)
k_B : Boltzmann's constant (1.38066×10^{-23} J K^{-1})
m : the chain length number
m_e : molality of electrolyte [mol kg^{-1}]
M_s : molecular weight of solvent [g mol^{-1}]
n : total number of mole [mol]
N_A : Avogadro's number (6.02205×10^{-23} mol^{-1})
R : gas constant (8.314 $Jmol^{-1}$ K^{-1})
T : absolute temperature [K]
u^0/k_B : temperature-independent dispersion energy of interaction between segments [K]
v : molar volume [m^3 mol^{-1}]
v^{00} : temperature-independent segment volume [mL mol^{-1}]
x_i : mole fraction of component i
Z : compressibility factor
Z_i : charge number of ionic species i

Greek Letters

Γ : MSA screening parameters [m^{-1}]
γ : activity coefficient
ε_0 : vacuum permittivity (8.85419×10^{-12} C^2 J^{-1} m^{-1})
$\varepsilon^{A_iB_j}$: energy of association [J]
σ_i : diameter of ionic species i
φ : fugacity coefficient
κ : Debye screening length [m^{-1}]
$\kappa^{A_iB_j}$: volume of association
μ : chemical potential [J mol^{-1}]
ν : stoichiometric number
OF : objective function defined by Eqs. (16) and (18)
Φ : osmotic coefficient

Subscripts

e : electrolyte
i : component i
ion : ion
MSA : mean spherical approximation theory
s : solvent
+ : cationic property of electrolyte
− : anionic property of electrolyte
± : mean ionic property of electrolyte

Superscripts

assoc : association contribution
cal : calculated properties
chain : chain contribution
disp : dispersion contribution
elec : electrolyte contribution
exp : experimental properties
hs : hard-sphere contribution
m : molality scale
res : residual
x : mole fraction
* : unsymmetrical normalization
∞ : infinite dilution properties

REFERENCES

1. J. Prausnitz, R. Lichtenthaler and E. de Azevedo, *Molecular thermodynamics of fluid-phase equilibria (3rd Ed.)*, Prentice Hall (1998).
2. G. M. Kontogeorgis and G. K. Folas, *Thermodynamic models for industrial applications*, John Wiley & Sons, Ltd. (2009).
3. L. Blum, *Mol. Phys.*, **30**, 1529 (1975).
4. L. Blum, *J. Stat. Phys.*, **18**, 451 (1978).
5. S. P. Tan, H. Adidharma and M. Radosz, *Ind. Eng. Chem. Res.*, **47**, 8063 (2008).
6. A. Haghtalab and S. H. Mazloumi, *Fluid Phase Equilib.*, **285**, 96 (2009).
7. C.-C. Chen and L. B. Evans, *AIChE J.*, **32**, 444 (1986).
8. K. S. Pitzer, *Activity coefficients in electrolyte solutions*, 2nd Ed., CRC Press (1991).
9. A. Haghtalab and J. H. Vera, *AIChE J.*, **34**, 803 (1988).
10. H. Planche and H. Renon, *The J. Phys. Chem.*, **85**, 3924 (1981).
11. J. A. Myers, S. I. Sandler and R. H. Wood, *Ind. Eng. Chem. Res.*, **41**, 3282 (2002).
12. M. A. Clarke and P. R. Bishnoi, *Fluid Phase Equilib.*, **220**, 21 (2004).
13. A. Haghtalab and S. H. Mazloumi, *Fluid Phase Equilib.*, **280**, 1 (2009).
14. W. G. Chapman, K. E. Gubbins, G. Jackson and M. Radosz, *Fluid Phase Equilib.*, **52**, 31 (1989).
15. A. Galindo, A. Gil-Villegas, G. Jackson and A. N. Burgess, *J. Phys. Chem. B*, **103**, 10272 (1999).
16. A. Gil-Villegas, A. Galindo and G. Jackson, *Mol. Phys.*, **99**, 531 (2001).
17. S. P. Tan, H. Adidharma and M. Radosz, *Ind. Eng. Chem. Res.*, **44**, 4442 (2005).
18. H. Adidharma and M. Radosz, *Ind. Eng. Chem. Res.*, **37**, 4453 (1998).
19. X. Ji, S. P. Tan, H. Adidharma and M. Radosz, *Ind. Eng. Chem. Res.*, **44**, 7584 (2005).
20. S. P. Tan, X. Ji, H. Adidharma and M. Radosz, *J. Phys. Chem. B*, **110**, 16694 (2006).

21. X. Ji, S. P. Tan, H. Adidharma and M. Radosz, *J. Phys. Chem. B*, **110**, 16700 (2006).
22. Z. Liu, W. Wang and Y. Li, *Fluid Phase Equilib.*, **227**, 147 (2005).
23. W. G. Chapman, K. E. Gubbins, G. Jackson and M. Radosz, *Ind. Eng. Chem. Res.*, **29**, 1709 (1990).
24. B. Behzadi, B. H. Patel, A. Galindo and C. Ghotbi, *Fluid Phase Equilib.*, **236**, 241 (2005).
25. H. Zhao, M. C. dos Ramos and C. McCabe, *J. Chem. Phys.*, **126** (2007).
26. H. Zhao and C. McCabe, *J. Chem. Phys.*, **125** (2006).
27. C. Held, L. F. Cameretti and G. Sadowski, *Fluid Phase Equilib.*, **270**, 87 (2008).
28. L. F. Cameretti, G. Sadowski and J. M. Mollerup, *Ind. Eng. Chem. Res.*, **44**, 3355 (2005).
29. S. Herzog, J. Gross and W. Arlt, *Fluid Phase Equilib.*, **297**, 23 (2010).
30. R. Shahriari, M. R. Dehghani and B. Behzadi, *Ind. Eng. Chem. Res.*, **51**, 10274 (2012).
31. S. H. Huang and M. Radosz, *Ind. Eng. Chem. Res.*, **29**, 2284 (1990).
32. S. H. Huang and M. Radosz, *Ind. Eng. Chem. Res.*, **30**, 1994 (1991).
33. M. S. Wertheim, *J. Stat. Phys.*, **35**, 19 (1984).
34. M. S. Wertheim, *J. Stat. Phys.*, **35**, 35 (1984).
35. M. S. Wertheim, *J. Stat. Phys.*, **42**, 459 (1986).
36. A. H. Harvey, T. W. Copeman and J. M. Prausnitz, *J. Phys. Chem.*, **92**, 6432 (1988).
37. A. A. Maryott and E. R. Smith, *Table of dielectric constants of pure liquids*, NBSCircular 514, U.S. Government Printing Office, Washington, DC (1951).
38. M. Valavi, M. R. Dehghani and R. Shahriari, *Fluid Phase Equilib.*, **344**, 92 (2013).
39. W.-B. Liu, Y.-G. Li and J.-F. Lu, *Ind. Eng. Chem. Res.*, **37**, 4183 (1998).
40. J.-F. Lu, Y.-X. Yu and Y.-G. Li, *Fluid Phase Equilib.*, **85**, 81 (1993).
41. Y. Li, *Tsinghua Science and Technology*, **9**, 444 (2004).
42. Y. Li, *Tsinghua Science and Technology*, **11**, 181 (2006).
43. L. L. Lee, *The J. Chem. Phys.*, **78**, 5270 (1983).
44. R. A. Robinson and R. H. Stokes, *Electrolyte solutions*, Dover Publications (2002).
45. R. A. Robinson and H. S. Harned, *Chem. Rev.*, **28**, 419 (1941).
46. P. Novotny and O. Sohnel, *J. Chem. Eng. Data*, **33**, 49 (1988).
47. J. C. Lagarias, J. A. Reeds, M. H. Wright and P. E. Wright, *SIAM J. on Optimization*, **9**, 112 (1998).
48. X. Ji and H. Adidharma, *Ind. Eng. Chem. Res.*, **46**, 4667 (2007).
49. S. S. Chen and A. Kreglewski, *Berichte der Bunsengesellschaft für physikalische Chemie*, **81**, 1048 (1977).

APPENDIX A

The SAFT-HR EoS [31,32] in terms of the residual Helmholtz energy is presented as follows:

$$\frac{A^{res}}{N_A k_B T}=\frac{A^{hs}}{N_A k_B T}+\frac{A^{disp}}{N_A k_B T}+\frac{A^{chain}}{N_A k_B T}+\frac{A^{assoc}}{N_A k_B T} \tag{A1}$$

the hard-sphere term is given by

$$\frac{A^{hs}}{N_A k_B T}=\frac{6}{\pi N_{Av}\rho}\left[\frac{\zeta_2^3+3\zeta_1\zeta_2\zeta_3-3\zeta_1\zeta_2\zeta_3^2}{\zeta_3(1-\zeta_3)^2}-\left(\zeta_0-\frac{\zeta_2^3}{\zeta_2^3}\right)\ln(1-\zeta_3)\right] \tag{A2}$$

where ζ_i is defined as

$$\zeta_i=\frac{\pi N_A\rho}{6}\sum x_i m_i d_{ii}^j, \qquad j=0, 1, 2, 3 \tag{A3}$$

$$d_{ii}=\sigma_i\left[1-0.12\exp\left(\frac{-3u^0}{kT}\right)\right] \tag{A4}$$

$$\sigma_i=\left(\nu^{00}\frac{6\tau}{\pi N_{AV}}\right)^{1/3} \tag{A5}$$

$$\tau=\pi\sqrt{2}/6 \tag{A6}$$

the dispersion term is as follows:

$$\frac{A^{disp}}{NKT}=m\sum_{i=1}^{4}\sum_{j=1}^{9}D_{ij}\left(\frac{u}{kT}\right)^i\left(\frac{\eta}{\tau}\right)^i \tag{A7}$$

$$\eta=\frac{\pi N_{Av}\rho}{6}\sum x_i m_i d_{ii}^3 \tag{A8}$$

D_{ij} universal constants are introduced by Chen and Kreglewski [49]. The vdW1 mixing rules for m and u/kT are used:

$$m=\sum_{i=1}^{N}x_i m_i \tag{A9}$$

$$\frac{u}{kT}=\frac{\sum_{i=1}^{N}\sum_{j=1}^{N}x_i x_j m_i m_j v_{ij}^0(u_{ij}/kT)}{\sum_{i=1}^{N}\sum_{j=1}^{N}x_i x_j m_i m_j v_{ij}^0} \tag{A10}$$

where

$$v_{ij}^0=\left\{\frac{1}{2}[(v_i^0)^{1/3}+(v_j^0)^{1/3}]\right\}^3 \tag{A11}$$

$$u_{ij}=(u_{ii}u_{jj})^{1/2}(1-k_{ij}) \tag{A12}$$

$$v_i^0=v_i^{00}\left[1-0.12\exp\left(\frac{-3u^0}{kT}\right)\right]^3 \tag{A13}$$

$$u_{ii}=u_i^0\left(1+\frac{e}{kT}\right) \tag{A14}$$

chain formation term is

$$\frac{A^{chain}}{NkT}=\sum_{i=1}^{N}x_i(1-m_i)\ln(g_{ii}^{hs}(d_{ii})) \tag{A15}$$

where

$$g_{ii}^{hs}(d_{ii})=\frac{1}{1-\zeta_3}+\frac{3d_{ii}}{2}\frac{\zeta_2}{(1-\zeta_3)^2}+2\left(\frac{d_{ii}}{2}\right)^2\frac{\zeta_2^2}{(1-\zeta_3)^3} \tag{A16}$$

Ultimately, the association term is as follows:

$$\frac{A^{assoc}}{NkT}=\sum_{i=1}^{N}x_i\left[\sum_{A_i}\left(X^{A_i}-\frac{X^{A_i}}{2}\right)+M_i/2\right] \tag{A17}$$

where X^{A_i}, the mole fraction of molecules i not bonded at site A is given by

$$X^{A_i}=\frac{1}{1+N_{Av}\sum_{j=1}x_j\sum_{B_j}\rho_j X^{B_j}\Delta^{A_iB_j}} \tag{A18}$$

the association strength $\Delta^{A_iB_j}$ is

$$\Delta^{A_iB_j} = g_{ij}(d_{ij})\left[\exp\frac{\varepsilon^{A_iB_j}}{kT} - 1\right]\sigma_{ij}^3\kappa^{A_iB_j} \tag{A19}$$

where

$$\sigma_{ij} = (\sigma_i + \sigma_j)/2 \tag{A20}$$

the radial distribution function $g_{ij}(d_{ij})$ is given by

$$g_{ij}(d_{ij}) = \frac{1}{1-\zeta_3} + \frac{3d_{ii}d_{jj}}{d_{ii}+d_{jj}}\frac{\zeta_2}{(1-\zeta_3)^2} + 2\left(\frac{d_{ii}d_{jj}}{d_{ii}+d_{jj}}\right)^2\frac{\zeta_2^2}{(1-\zeta_3)^3} \tag{A21}$$